



Porosity and fire resistance of fly ash based geopolymer

S. Alehyen, M. Zerzouri, M. ELalouani, M. EL Achouri, M. Taibi

*Mohammed V University –Ecole Normale Supérieure-Rabat-Morocco
Laboratoire de Physico-Chimie des Matériaux Inorganiques et Organiques
Ecole Normale Supérieure-Rabat*

Received, 26 Apr 2017
Revised 06 June 2017,
Accepted 10 June 2017

Keywords

- ✓ Fly ash
- ✓ Geopolymer
- ✓ Porosity
- ✓ BJH method
- ✓ BET method
- ✓ Thermal stability
- ✓ Fire resistance
- ✓ Microstructural changes.

alehyensali@yahoo.fr

Abstract

The fly ash based Geopolymer (FA-GP) is a promising binder manufactured by activation of Jorf Lasfer's fly ash with a highly alkaline activating solution. The FA-GP prepared were characterized by several analytical methods. The present work reports the experimental results of the porosity and fire resistance studies of fly ash based geopolymer FA-GP binder and Ordinary Portland Cement (OPC) cement for comparison. The porosity studies of FA-GP and OPC cement pastes were determined using N₂ adsorption/ desorption plots. Surface areas were calculated from the isotherm data using the (BET) method. The total pore volume and micropore volume of the samples were calculated using t-plot analysis. The Barrett-Joyner-Halenda (BJH) method was used to obtain pore size distribution curves. The result shows that the FA-GP pores had a significant proportion of micropores whilst OPC cement pores were predominantly mesopores. The thermal and fire resistance properties were determined by investigation of thermal stability up to 1000°C of FA-GP and OPC paste for comparison. The effect of heat treatment on the FA-GP and OPC pastes heated at elevated temperature (600°C, 800°C and 1000°C) was studied and the fire resistance of samples pastes is evaluated by visual observation, weight loss, and microstructural change after thermal treatment at high temperature. The microstructural changes before and after heat exposure were evaluated using FT-IR, DRX and SEM analysis. The results show that the FA-GP possesses superior fire resistance compared to OPC cement. The excellent fire resistance performance of FA-GP is due to their ceramic-like characteristics.

1. Introduction

The first and foremost drive for the research and commercialization of geopolymer technology has been the need to find alternative cleaner materials to substitute Ordinary Portland Cement OPC as a construction material. Studies have shown that for every tonne of cement produced, 0.55 tonnes of chemical CO₂ is generated, which is 8 times higher than emissions resulting from metallurgical activities [1]. Geopolymers are a very promising kind of material, since they have been shown to offer an environmentally friendly, technically competitive alternative to ordinary Portland cement (OPC) [2–4]. Geopolymer binders possess many advanced properties such as fast setting, excellent bond strength, good long-term properties and durability [5], good ability to immobilize toxic metals and better fire and acid resistance [6-8]

The term 'Geopolymer' was first applied to amorphous aluminosilicate binders formed through hydrothermal synthesis of aluminosilicates in the presence of concentrated alkaline or alkaline silicate solutions by Davidovits [9]. Early geopolymer materials set rapidly at low temperatures, only a few hours at 30 °C, or a few minutes at 85 °C, or a few seconds in a microwave oven [10].

They display compressive strength as high as 60 MPa after just one day of curing and the strength will continue to increase up to 100 MPa. They also exhibit a 4-7 Mohs hardness, and are thermally stable upon subjection to very high temperature (1000-1200 °C), where all organic resins or cement fail to perform. These findings have made geopolymers potentially useful for ceramic, refractory lining materials, as well as for building materials [10].

There are two main constituents of geopolymers, namely the source materials and the alkaline liquids. The source materials for geopolymers based on alumino-silicate should be rich in silicon (Si) and aluminium (Al). These could be natural minerals such as kaolinite, clays, micas, andalusite, spinel, etc whose empirical formula contains Si, Al, and oxygen (O) [10]. Alternatively, by-product materials such as fly ash, silica fume, slag, rice-husk ash, red mud, etc could be used as raw materials [11-13]. The choice of the source materials for making geopolymers depends on several factors such as availability, cost and type of application. The alkaline liquids are from soluble alkali metals that are usually sodium or potassium based.

The geopolymeric materials possess high fire resistance and can enhance the fire/heat resistant performance of structures. Moreover, most organic matrix cannot support the temperature more than 200°C and will issue poison gas when exposed to fire. Therefore, there is an urgent necessity to enhance the fire/heat resistant performance of structures. Geopolymer concrete, coating, and matrix may resolve these problems. The geopolymers discovered recently are reported to possess excellent fire resistant performance due to their ceramic like characteristics. Geopolymeric cement was superior to Portland cement in terms of heat and fire resistance, as the Portland cement experienced a rapid deterioration in compressive strength at 300°C, whereas the geopolymeric cements were stable up to 600°C [14-15].

The objective of this work is the valorization of fly ash generated by the Moroccan thermal power plants by their use in the field of building materials and civil engineering. The study focuses on porosity and fire resistance properties of geopolymer binders based on Moroccan fly ash. FA-GP were synthesized by alkaline activation of fly ash generated by Jorf Lasfar power plant in Morocco. The composition, structure and microstructure of FA-GP binder were investigated using several analytical methods. The Porosity measurements of FA-GP and OPC pastes were undertaken using nitrogen adsorption / desorption method. Fire resistance properties of FA-GP and OPC pastes were evaluated by visual observation, weight loss and microstructural change after heat treatment.

2. Experimental

2.1. Fly ash

Geopolymer samples were prepared from fly ash supplied by Jorf Lasfar power plant in Morocco. The chemical composition of fly ash determined by Fluorescence X-Ray Spectroscopy is given in Table 1. The fly ash is classified as ASTM Class F fly ash. The size distribution curve of fly ash obtained by granulometric analysis using laser diffraction is shown in figure 1. It contains 50% particles smaller than 40,6 nm. The BET surface area of fly ash is 3,6 m²/g.

Table 1 : Chemical composition of Jorf Lasfar fly ash

Constituent	LOI	SiO₂	Al₂O₃	Fe₂O₃	CaO	K₂O	Na₂O	TiO₂	SO₃	P₂O₅	MgO
%	7,12	52,5	30,2	2,94	0,822	2,08	0,719	1,03	0,787	0,203	1,23
Constituent	Rb	SrO	BaO	ZrO₂	Cr₂O₃	Nb₂O₅	CuO	ZnO	NiO	I	PbO
%	0,0694	0,0518	0,0484	0,0382	0,0287	0,0156	0,0137	0,0126	0,0116	0,0109	0,0146

*LOI :Loss of ignition

2.2 Preparation of specimens

2.2.1 Geopolymer paste

The mixture of sodium hydroxide (12 M NaOH) and sodium silicate was used as an activator for preparation of FA-GP specimens. Na₂SiO₃ powder (18% Na₂O and 63% SiO₂) is purchased from Riedel –de-Haen and NaOH pellets of purity > 97% from Fluka. Sodium silicate to sodium hydroxide ratio was 2, 5:1. The FA-GP were prepared by mixing the activator (sodium hydroxide and sodium silicate) and fly ash in a ratio of 0.4. After mixing, the geopolymer pastes were cast in a cylindrical plastic moulds, and left for 24h at the temperature of 70°C. After demoulding, the specimens were left to air-dry in the laboratory until the day of test.

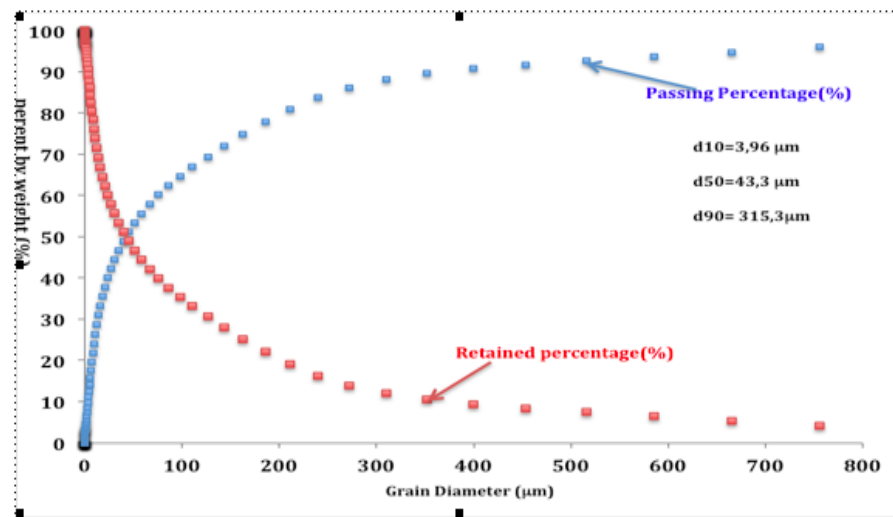


Figure1 : The Particle Size Distribution (PSD) of fly ash obtained by laser diffraction

2.2.2 Cement paste

The cement pastes are made by mixing a cement CEM II 32, 5 R and water. The water / cement ratio is equal to 0.5. The samples were thoroughly mixed for two minutes and then allowed to hydrate in air tight plastic containers.

2.3 Characterization Methods

Fluorescence X-Ray analysis of samples was performed using wavelength dispersive (WDXRF) spectrometer Axios type. The mineral composition of fly ash, geopolymer and cement pastes samples was determined by X-Ray diffraction (XRD) using Siemens/Bruker D5000 X-ray powder diffraction system equipped with CuK radiation. The Fourier transform infrared spectroscopy (FTIR) spectra of materials samples were recorded using ATR Alpha platinum FT-IR Spectrometer.

²⁹ Si MAS-NMR spectroscopic characterization was conducted with Bruker apparatus, model AvanceIII 600MHz. The spectrometer used has a main field magnetic 14 Tesla. The measurements were taken at laboratory temperature with TMS as the external standard.

Microstructural investigations of the geopolymer paste were carried out using the FEI quanta 450 FEG focused- ion-beam system, equipped with an EDAX Genesis energy dispersive spectrometer (EDS) at Moroccan Foundation for Advanced Science, Innovation and Research (MASCIR). Particle size analysis of raw fly ashes was determined by dynamic laser scattering (Matersizer- Malvern Instruments, UK) at MASCIR foundation.

2.4 N2 adsorption/desorption porosimetry

N2 adsorption/desorption plots of powdered specimens were carried out with a Micromeritics "3Flex 3500" analyzer under continuous adsorption conditions. Prior to these measurements, samples (about 1 g) were heated at 400 °C for 10 h and outgassed to 10–2 Torr. Gas adsorption analysis in the relative pressure range of 0.05 to 0.3 was used to determine the total specific area. Surface areas were calculated with an accuracy of 10%, from the isotherm data using the Brunauer, Emmet and Teller (1938) (BET) method [16]. The total pore volume and micropore volume of the samples were calculated using t-plot analysis. The Barrett-Joyner-Halenda (BJH) method was used to obtain pore size distribution curves [17].

2.5 Thermal and Fire resistance Properties

Fire resistance properties were determined by studies of thermal stability and themal behavior after heat exposure of FA-GP and OPC pastes for comparison.

2.5.1 Thermal Sability

The thermal stability of FA-GP and OPC paste was studied by Differential Scanning Calorimetry (DSC). The DSC is performed using DSC SETARAM devise and the curves were recorded under argon atmosphere in the temperature range between 30 and 800°C.

2.5.2 Fire resistance

Muffle furnace was used for this study. Specimens were subjected to heat at temperatures of 600°C, 800°C and 1000°C at an incremental rate of 4°C per minute from room temperature. The temperature was sustained for 2 hours. Then the specimens were allowed to cool down for 24 hours at room temperature inside the furnace. The effect of heat treatment on the FA-GP and OPC pastes heated at elevated temperature (600°C, 800°C, 1000°C) was studied and the fire resistance of samples pastes is evaluated by visual observation, weight loss, and microstructural change after thermal treatment at high temperature. The microstructural changes before and after heat exposure was evaluated using FT-IR, DRX and SEM analysis.

3. Results and Discussion

3-1 Characterization of FA-GP

3-1-1 FX analysis

The chemical composition of geopolymer is given in Table 2. The major constituents of fly ash based geopolymer were the silicon, the sodium and aluminum oxides. Indeed, these components represented 79% of the total mass of geopolymer.

Table 2 : Chemical composition of FA- geopolymer

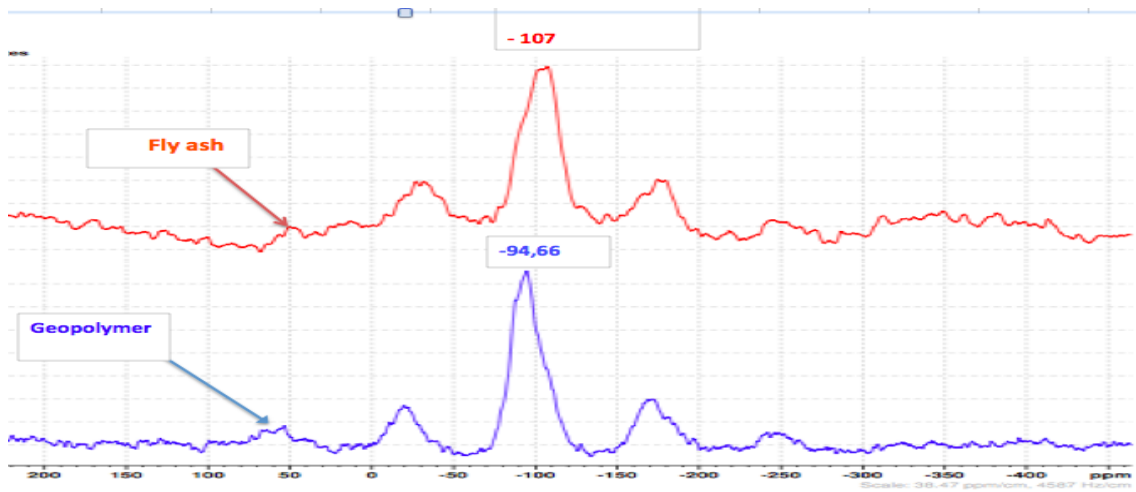
Constituent	LOI	SiO₂	Na₂O	Al₂O₃	Fe₂O₃	K₂O	K₂O	TiO₂	MgO	CaO	SO₃
%	5,82	37,8	28,3	15,9	4,67	2,65	0,719	1,58	1,18	1,15	0,37
Costituent	P₂O₅	SrO	BaO	ZrO₂	CuO	Nb₂O₅	CuO	ZnO	Rb	I	
%	0,1	0,0896	0,0882	0,0666	0,0345	0,0341	0,0137	0,0338	0,027	0,025	

3.1.2 ²⁹Si RMN MAS analysis

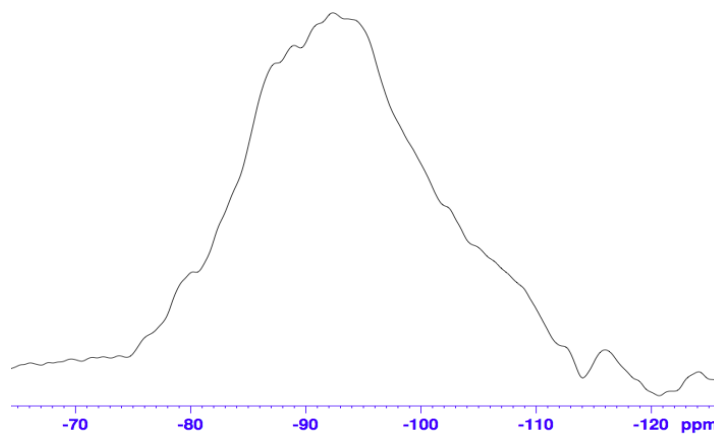
In ²⁹Si MAS-NMR spectroscopy, the chemical shift $\delta(^{29}\text{Si})$ depends on the local environment of the ²⁹Si nucleus. The explanatory investigation by Lippman et al [18] on silicates with known molecular structure showed that the ²⁹Si chemical shift mainly depends on the degree of condensation of SiO₄ unit, with increasing condensation corresponding to a high-field shift, more negative $\delta(^{29}\text{Si})$. Q_n(mAl) unit is the conventional notation to describe the structural units in aluminosilicates, where « n » represents the covalence number of the silicon center and « m » the number of Al surrounding one SiO₄ unit. The chemical structures of all possible Q_n(mAl) units are given by Klinowski [19]. In this way, if n = 0, 1, 2, 3 and 4, then silicon is respectively in isolated mono-group (Q₀), in disilicates and chain end group (Q₁), in middle group in chains (Q₂), in sheets sites (Q₃) and in three-dimensional cross-linked site (Q₄). The letter « m » represents the number of aluminium atoms in the first covalence sphere of silicon, the number of Si-O-Al, sialate unit.

The ²⁹Si RMN MAS spectra of FA and FA-GP is illustrated in figure 2 a. The chemical shift equal to -107 ppm identified in ²⁹Si NMR MAS spectra of FA is the most important and is attributed to the tetrahedral [SiO₄]⁴⁻ coordination Q₄(0Al) [19-21]. A different situation was detected in the fly ash based geopolymers paste. The main shift equal to -94, 5 ppm corresponding to the Q₄(2Al) and Q₄(3Al) were found. The shift equal to -107 ppm corresponding to the Q₄(0Al) coordination was less represented, which points to the Al penetration into the [SiO₄]⁴⁻ skeleton. This interpretation of the NMR spectra is also shared by other workers [20-21]. The NMR spectra of fly ash based geopolymer illustrated in Figure 2 b shows peaks at -80, -86, -89, -92,5, -94 and -103 ppm corresponding respectively to Q₁(0Al), Q₄(3Al), Q₄(3Al), Q₄(2Al) and Q₄(1Al) respectively according to Klinowsky [19].

The high intensities of signals obtained at -93 and -96 ppm means that the Q₄(2Al) and Q₄(3Al) units prevailed. This result agrees with that found by Davidovits [9] which proposed the structural model of geopolymer shown in Figure 3. The basic building block of a geopolymer is a tetrahedral silicon and aluminium bonded through sharing of oxygen atoms. Only Al^{IV} is found to be suitable to replace Si^{IV} in a tetrahedral arrangement. The basic monomer unit is a sialate, with Mn(-(SiO₂)_z-AlO₂)_n.wH₂O to be the empirical formula for polysialates, where z is 1, 2, 3; M is a monovalent cation, such as potassium or sodium; and n is the degree of polycondensation [9-10].



29
Figure 2 a : Si MAS NMR spectrum of fly ash and fly ash based geopolymer



29
Figure 2 b : Si MAS NMR spectrum of fly ash based geopolymer

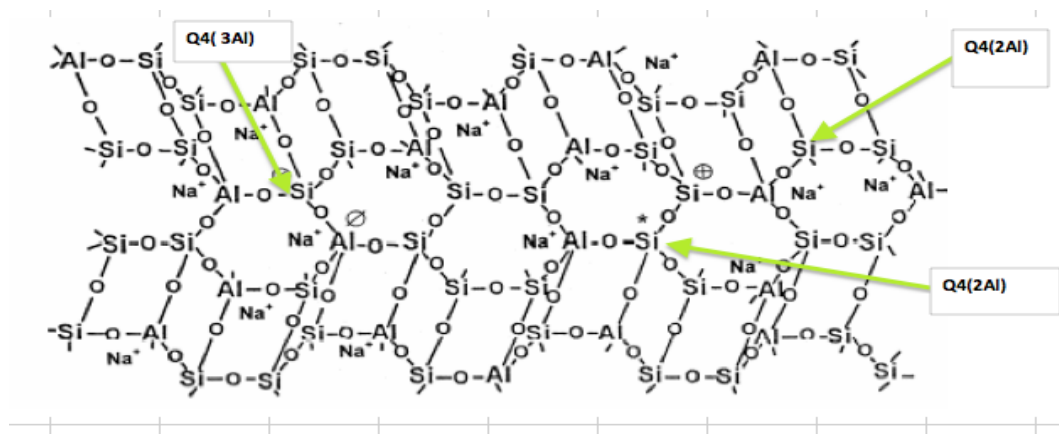


Figure 3 : Conceptual model of geopolymer proposed by Davidovits [9-10]

3.1.3 SEM and EDS micro analysis

3.1.3.1 FA-GP SEM

Figures 4 illustrate the SEM-determined microstructure characteristics of the prepared fly ash-based geopolymers. The microstructure of FA-based geopolymers is a porous, heterogeneous mixture of non- or partly-reacted fly ash grains, residual alkaline precipitates, and geopolymer gel. Figure 4 b shows SEM micrograph of non-active spherical ash in the geopolymer binder and Figure 4 c shows the interface between geopolymer binder and fly ash particles.

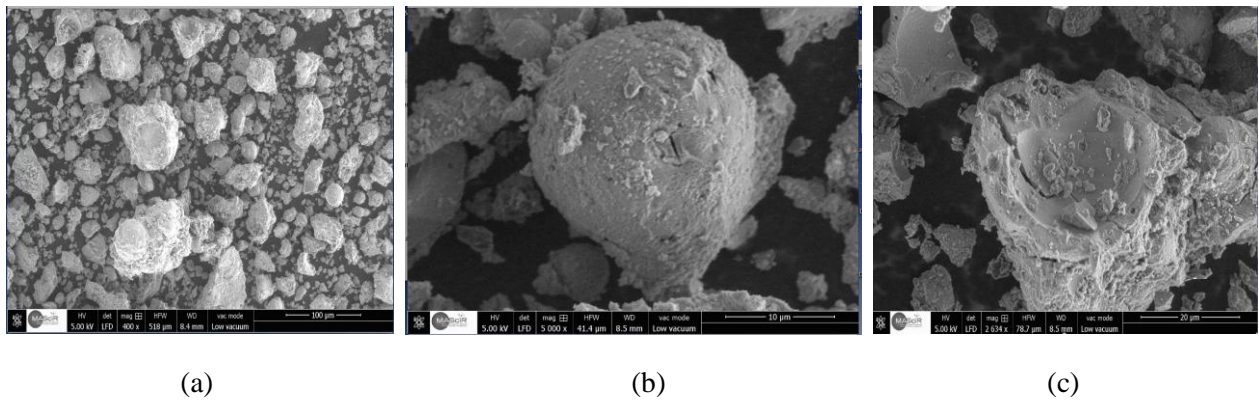


Figure 4 : SEM micrographs of fly ash based geopolymer

3.1.3.2 FA-GP EDXS microanalysis

The geopolymer paste consists of a gel phase and unreacted fly-ash particles. Figure 5 illustrates the results of an EDS analysis of the gel phase in geopolymer matrix in the selected area and shows that the main constituent of the geopolymer are O, Si, Na and Al. In addition to the major elements (Na, K, Al, O, Si), constituting the geopolymer binders, the elements of Ca and Fe are also present. It is observed that the Si/Al ratio is close 1 in the gel matrix in the selected area. Therefore, the gel matrix have a polysialate structure [9].

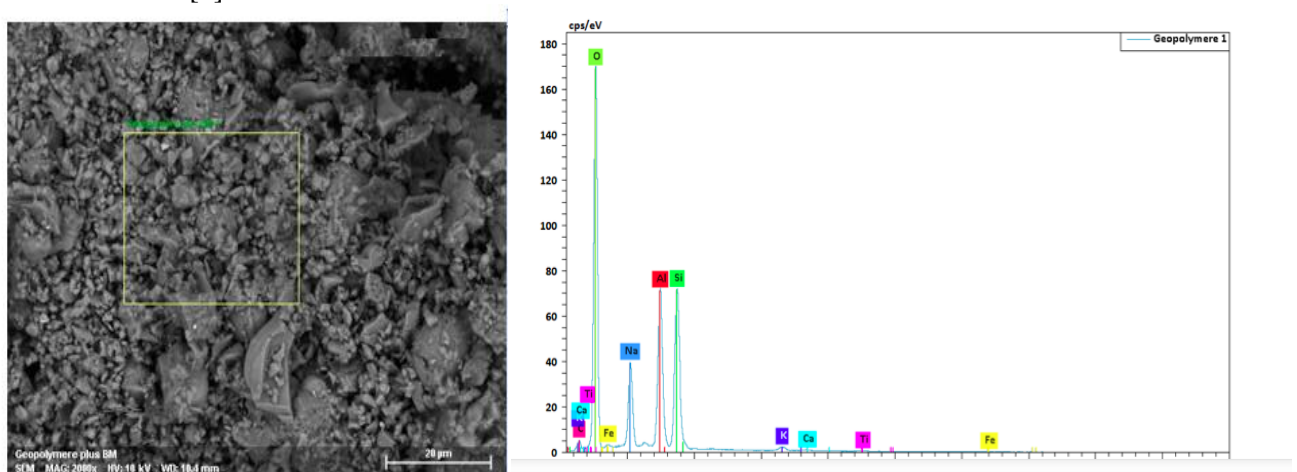


Figure 5: Qualitative EDXS analysis of selected area in the geopolymer matrix

3.2 Nitrogen adsorption Porosity measurement

The porosity is the proportion of the total volume occupied by pores. If the pores are interconnected, then the permeability tends to be high and the porosity is high, vice versa if the porosity is low and the pores are disconnected, then the permeability is relatively low [23]. Nowadays, no experimental method allows to measure the pore structure of cementitious materials completely. So far, numerous experimental methods have been developed to measure or assess the pore structure and the most widely used methods include the mercury intrusion porosimetry (MIP) and nitrogen adsorption/desorption methods. The gas adsorption method has also been used to identify the pore structure of cement-based materials for decades [23–25]. On the basis of the adsorbed gas quantity, the internal surface area of pores can be evaluated from the Langmuir monomolecular layer theory or the BET multilayer adsorption theory. Furthermore, the pore size distribution can be obtained using Barrett–Joyner– Halenda (BJH) interpretation based on capillary condensation [24]. The pore structure of samples is characterized by the total porosity, pore size distribution (PSD), pore internal surface area as well as characteristic pore sizes. In order to gain more insight into the pore size distribution, the measured pore distribution is divided into four size ranges: gel micropores (< 4.5 nm), mesopores (4.5–50 nm), middle capillary pores (50–100nm) and large capillary pores (> 100 nm), according to Metha and Monteiro [23].

In this study, Brunauer-Emmett-Teller surface (BET) method using N₂ adsorption was used to determine the pore structure of the fly ash based geopolymer prepared and the commercial portland cement

OPC for comparison. Table 3 shows the parameters that were determined by nitrogen sorption, while Figure 6 (a, b) shows the representative pore size distribution for FA-GP geopolymer and OPC pastes.

Table 3: Parameters obtained by the nitrogen Adsorption method for FA-GP and OPC pastes

Parameters		Geopolymer FA-GP	Cement OPC
Surface Area	Single point surface area	2,4883	19,2311
	BET Surface Area: (m ² /g)	2,5080	19,3677
	t-Plot Micropore Area(m ² /g)	0,3743	4,0443
	t-Plot External Surface Area(m ² /g)	2 ,1338	15,3235
	BJH Adsorption cumulative surface area of pores (m ² /g)	2,156	13,4348
	BJH Desorption cumulative surface area of pores (m ² /g)	1,8533	13,9018
	D-H Adsorption cumulative surface area of pores (m ² /g)	2.063	12,7829
	D-H Desorption cumulative surface area of pores (m ² /g)	1,7790	13,3106
Pores Volume	Maximum pore volume at $p/p^{\circ} = 0,148548356$ (cm ³ /g) <u>(Horvath-Kawazoe method)</u>	0,001037	0,001994
	Cumulative pore volume of pores (cm ³ /g) (MP-method)	0,000076	0,017532
Pore size	Median pore size (nm)	1,1738	5,252

According to Table 3, the fly ash based geopolymers show lower average pore sizes, lower total pore volumes and lower surface area of pores than OPC paste samples. The average pore size (1,17 nm) obtained for the fly ash based geopolymer is lesser than 4,5 nm means that the geopolymeric matrix is predominantly a microporous material. On the other hand, the average pore size for OPC cement II paste (5,2 nm) is greater than 4,5 nm, indicating that the cement tested are predominantly composed of mesopores. The small pores volume and surface area for the FA-GP geopolymer indicates that the geopolymer matrix is dense, which means that its permeability will be low and consequently its durability will be high [22].

Figure 6 (a,b) shows that the pore size distribution of the geopolymer and OPC pastes are unimodally distributed. Figure 6 a and b presents a clear maximum at 3 nm and 3,8 nm respectively meaning that the creation of mesoporosity (radius > 4,5 nm) is more significant in CEM II than fly ash based geopolymer materials. Indeed, the creation of mesoporosity influences the evolution of the surface area, the more the creation of mesoporosity is significant, the more the surface area increases. This fact explained the greater BET N₂ obtained in the case of cement paste.

Fly ash based geopolymer paste showed considerably lower pore volume than OPC paste meaning that FA-GP paste is more compacted and dense than the cement paste tested. Therefore, the porosity of FA-GP is smaller than that of OPC cement studied. Since the porosity is inversely proportional to the

mechanical strength, it can be expected that the mechanical strength of the geopolymer will be greater than that of OPC cement [26-27]. Indeed, Porosity has been shown to display an inverse relationship to compressive strength, with reduction of porosity leading to increases in compressive strength of a material [25 -29].

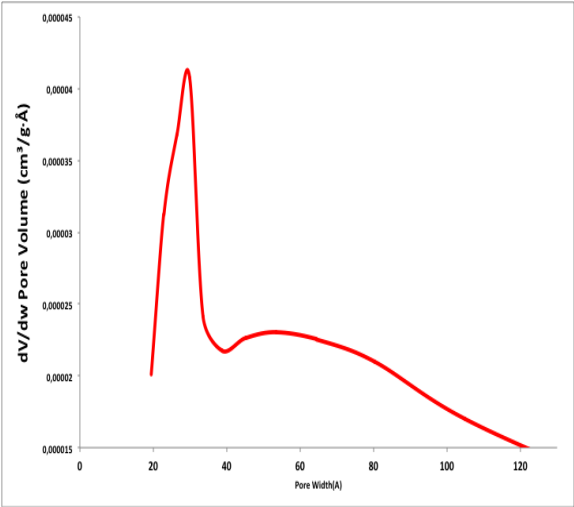


Figure 6a: Pore size distribution in FA –GP paste.

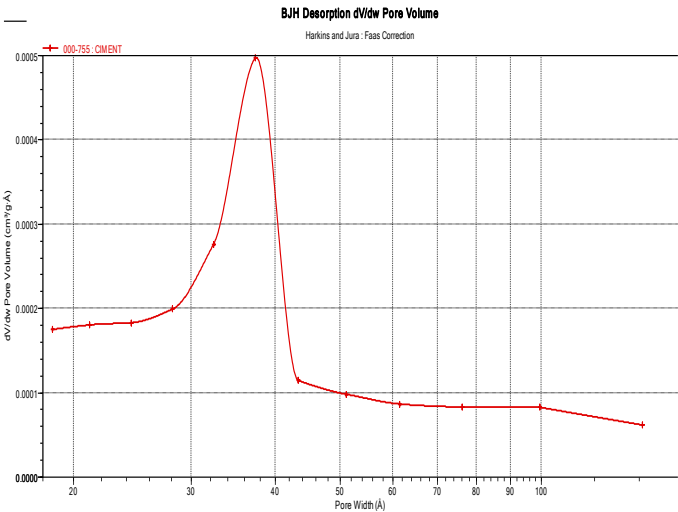


Figure 6b: Pore size distribution in OPC paste

3.3 Thermal and Fire resistance Properties

The thermal Stability of FA-GP and OPC paste was undertaken using DSC measurements. Fire resistance properties of fly ash based geopolymer FA-GP and OPC pastes were evaluated by means visual change, weight loss and microstructural changes after heat treatment at 600°C, 800°C and 1000°C.

3.3.1 Thermal stability by Differential Scanning Calorimetry (DSC)

The thermal stability was performed using Differential Scanning Calorimetry analysis. The DSC curves of fly ash based geopolymer and OPC pastes were illustrated in figure 7.

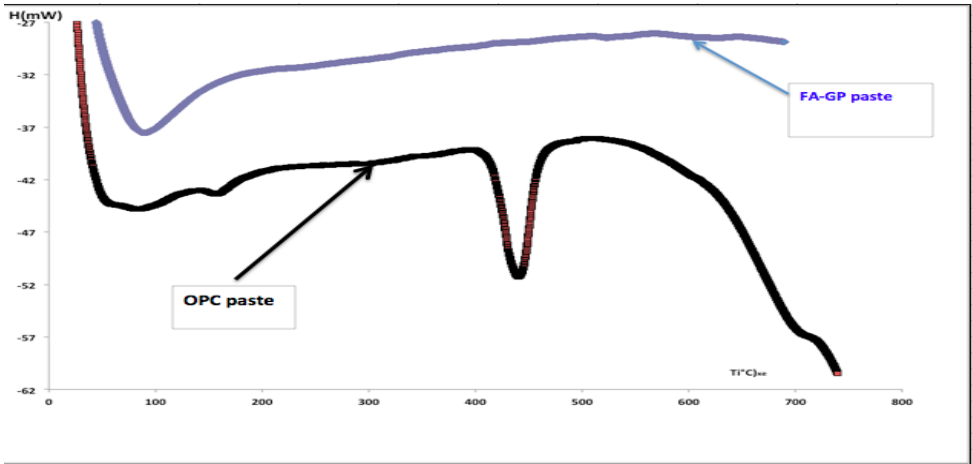


Figure 7: DSC curve of fly ash based geopolymer FA-GP and OPC pastes.

DSC curve of the FA-GP geopolymer samples shows an endothermic peak between 65 and 165°C centered at 85 °C. It is associated to removal of water. This fact indicates the presence of the weakly bound water molecules that were adsorbed on the surface or trapped in the large cavities between the rings of the geopolymeric products. The FA-GP exhibits a high thermal stability at elevated temperature in the range [50,800 °C]. This result agrees those of Cheng and Chiu [30]. In the opposite, the DSC curve of cement paste presents several endothermal pics which are related to dehydration of OPC paste. Indeed, Calcium silicate hydrate (CSH) and calcium hydroxide Potlandite (CH) are the main hydration phases which dominate the properties of Portland cement paste.

The dehydration of Portland cement paste is due to dehydration of CSH and CH [31]. The temperature range corresponds to the dehydration of CSH is about from 105 to 1000°C [32]. The temperature range corresponds to the dehydration of CH is about from 400 to 550°C. Carbonated phases decompose in a large temperature interval from 500 to 800 °C. The DSC curves clearly show that the FA-GP geopolymer is more thermally stable than the OPC cement paste.

3.3.2 Visual change after heat treatment

Figure 8 shows the fly ash geopolymers and OPC pastes samples prepared before and after heating at 600°C, 800°C and 1000°C. After heat treatment exposure, the color of the geopolymer samples became slight lighting. Macro-cracks have been observed on the surface of the OPC samples after 600° C. Geopolymer binders are well conserved after high temperature exposure, it shows no cracks on their surface. The OPC samples were completely destroyed after heating at 1000° C. All geopolymers exposed to high temperature retained their shape up to 1000 °C without showing any cracks or dimensional change. This was supported by Skvara et al. [33] for fly ash geopolymers.

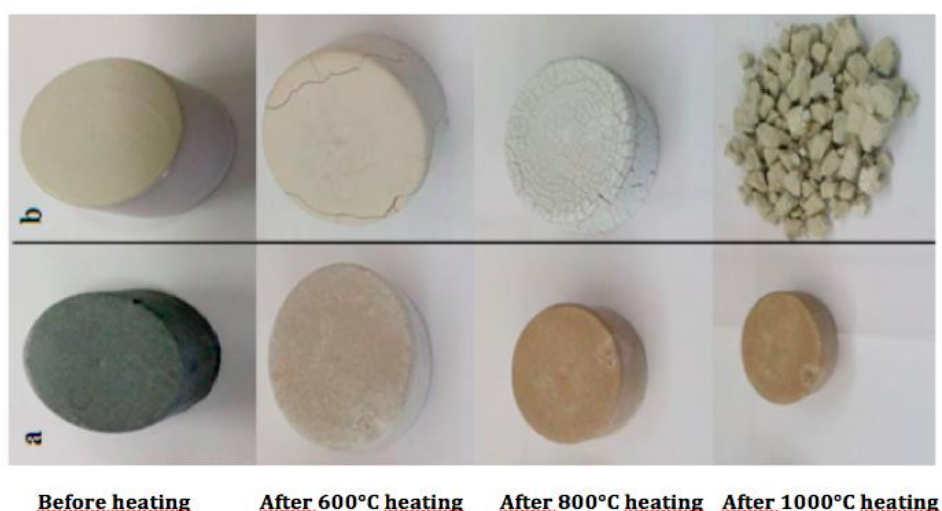


Figure 8: Samples of geopolymer (a) and OPC (b) before and after heat exposure

3.3.3 Weight loss measurements

Table 4 summarises the weight loss of FA-GP and OPC pastes at different temperatures. According to this Table, higher exposing temperature resulted in a higher mass loss. For fly ash geopolymer paste, little mass change was observed after 600 °C up to 1000 °C, which was also observed by Zhang et al [34] in metakaolin-fly ash based geopolymers. The weight loss of FA-GP were smaller than that of OPC paste as found by Luna-Galiano et al [35]. According to the authors, OPC samples had a higher mass loss than geopolymers and therefore greater degradation with rising temperature. The OPC paste was totally damage at elevated temperature [36-37] due to evaporation of water and decomposition of hydrate products [35, 38]. The weight loss measurements are consistent with the results of DSC analysis.

Table 4: Weight loss of FA-GP and OPC pastes

Temperature (°C)	600	800	1000
FA-GP paste Weight loss%	18,80	20,5	20,7
OPC paste Weight loss%	13,35	20	33,9

3.3.4 Microstructural Change by FTIR analysis

Figures 9 a and b represent the FTIR spectra of fly ash based geopolymers and OPC paste respectively before and after exposure to elevated temperature. According to figure 9 a, Fly ash based geopolymer at ambient temperature before heat exposure showed main broad band at 1000 cm⁻¹, corresponding to the asymmetrical stretching vibration of Si-O-Si and Si-O-Al.

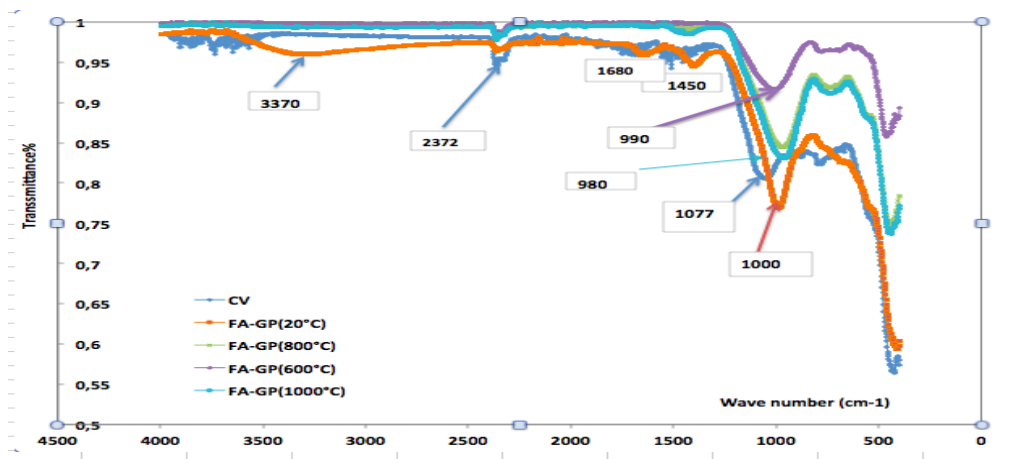


Figure 9 a: FT-IR spectra of flyash geopolymer before and after heat treatment

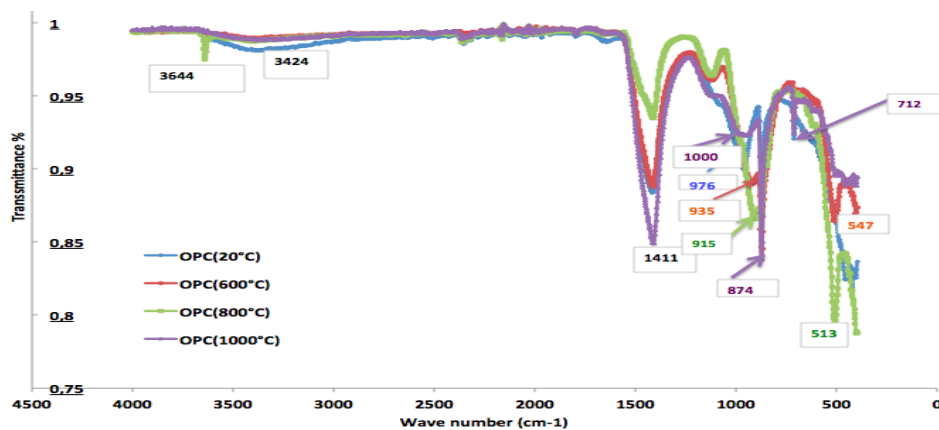


Figure 9b : FT-IR spectra of OPC before and after heat treatment at 600,800 and 1000°C.

The other absorption bands at 3372 cm^{-1} and 1680 cm^{-1} were attributed to the OH stretching vibration and bending vibration, respectively. The band at 1450 cm^{-1} was attributed to the CO_3^{2-} ion resulted from the reaction of atmospheric CO_2 with residual sodium content [39]. The band at 1000 cm^{-1} are particularly sensitive to geopolymer gel structure indicating that formation of geopolymers took place in the reaction. Amorphous SiO_2 and Al_2O_3 are transformed to aluminosilicates gel during the reaction between fly ash and NaOH. Their vibration bands in the IR spectrum are replaced by a single band around 100 cm^{-1} , characteristic of Si–O–Al bonds in TO_4 tetrahedra [40]. The peak at 1000 cm^{-1} attributed to the formation of new amorphous aluminosilicate gel phase suggests depolymerisation and structural reorganization of the amorphous phases in the alkali-activated fly ash [41]. With increasing temperature, the peak at 1000 shift to more lower frequencies indicating that the geopolymerization reaction take place at high temperature between the residual unreacted fly ash present in the geopolymer sample and alkaline solution. The shift is interpreted as the result of a further aluminum Al penetration into the original structure of the Si-O-Si network, similar to those bands which were detected in the zeolites. A structural reorganization occurs in which aluminum ions are incorporated into the SiO_4 tetrahedra, forming more Si-O-Al bands in the geopolymer network [42]. With increasing temperature, the sodium carbonate band disappeared as it started to decompose at 400 °C. Similar to many other geopolymers exposed to heat treatment [43], the bands at 3372 cm^{-1} and 1680 cm^{-1} lowered in intensity with increasing temperature exposure, indicating fully dehydration of geopolymers.

FT-IR spectra of cement pastes heated in the temperature range 20-1000°C, are represented in figure 10 b. A wide IR band obtained at 20°C at 976 cm^{-1} , is due to the silicate phases [43-45]. Along with the increasing temperature to 1000°C, the maximum peak due to silicate phases is moved towards lower wave numbers (935 cm^{-1} at 600°C, 915 cm^{-1} at 800°C and 874 cm^{-1} at 1000°C). A shift of the observed IR band at 976 cm^{-1} towards lower wave numbers is attributed to decomposition of the cement gel C-S-H [45]. The change in the structure of cement gel is due to the liberation of chemically bounded water. With increasing

the temperature, the wide band due to silicate phases at 976 cm⁻¹ splits into three bands at 1000, 874 and 712 cm⁻¹. The appearance of new bands evidences a transformation of the gel structure and the formation of ordered phases, similar to the structure of C2S [44]. The appearance of new band at 515 cm⁻¹ confirm the presence of C2S and decomposition of C-S-H gel of cement paste heated at high temperature. The comparative study of microstructural change by FT-IR analysis confirmed the high thermal stability of fly ash based Geopolymer and low thermal stability of cement paste mainly due to decomposition of the C-S-H gel, the main binding product in the cement matrix due to evaporation of water.

3.3.5 Microstructural change by XRD analysis

Figure 10 a shows the XRD pattern of FA-GP paste, while Figure 10 b presents XRD spectra of OPC cement paste before and after heat treatment. XRD pattern of fly ash based geopolymer illustrated in figure 10 a shows that the geopolymer materials are prevalingly of X-ray amorphous character where the diffraction crystals were those of the original fly ash materials: mullite and quartz. The broad peak observed around 20-40° which is attributed to the formation of amorphous aluminosilicate gel N-A-S-H, which has been identified as the primary reaction product of geopolymeric materials [46].

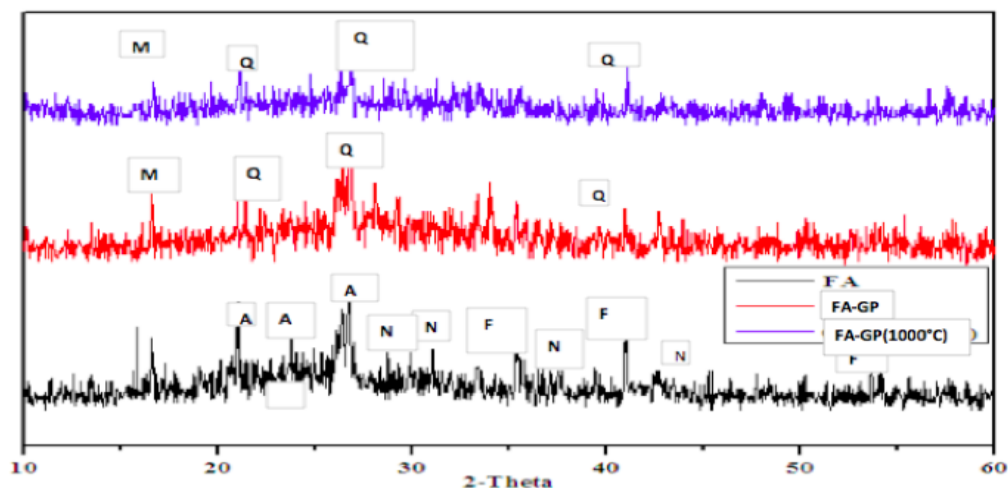


Figure 10 a : XRD pattern of fly ash (FA) and fly ash based geopolymer (FA-GP) before and after heating at 1000 °C . A :Albite ; F :Faujasite ; N :Nepheline ; Q : Quartz ; M : Mullite

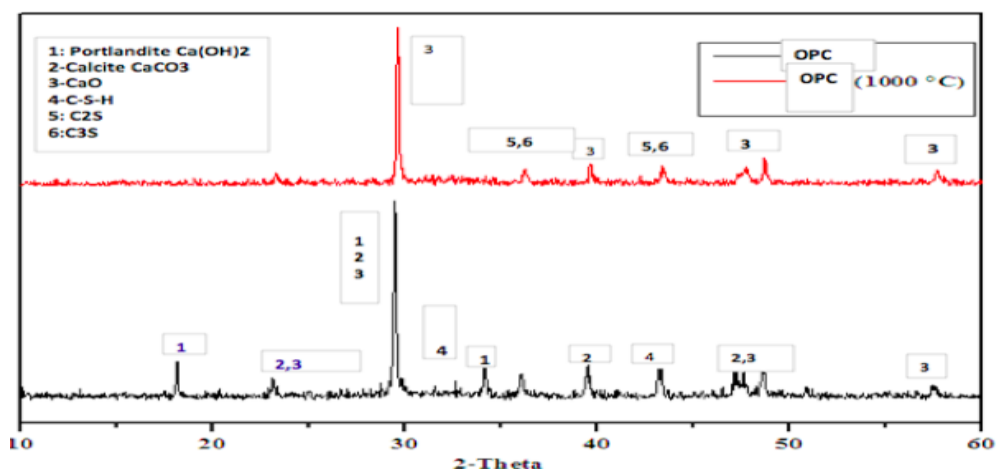


Figure 10 b : XRD pattern of OPC before and after heating at 1000°C.

Indded, the structure of geopolymers is often described by several autorsbroadly by the term ‘X-ray amorphous’ [47-48]. Slight changes in intensity are observed in this halo with increasing temperaturebut are difficult to quantify. The geopolymer binder remains amorphous over a wide range of temperatures; however, at temperatures over 1000°C, several crystalline products have been observed according to the chemical composition of the original geopolymer. The elevated temperature increased the propensity towards

the formation of stable crystalline phases. The characteristic peaks of Albite ($\text{NaAlSi}_3\text{O}_8$), nepheline ($\text{NaAlSi}_3\text{O}_4$) and Faujasite can be observed in the DRX spectra of FA-GP after heat exposure at 1000°C as shown in figure 10 a. This result agree with the finding of Rovnaník et al [48] which have observed the formation of nepheline ($\text{NaAlSi}_3\text{O}_4$), jadeite ($\text{NaAlSi}_2\text{O}_6$), and albite ($\text{NaAlSi}_3\text{O}_8$) in Na-based geopolymers. Formation of nepheline, anorthite and cristobalite have been reported in geopolymers at higher temperature exposure according to some studies [49-50]. In general, the crystallization would most probably enhance the mechanical properties of geopolymers [50]. The presence of kalsilite (KAlSiO_4) and leucite (KAlSi_2O_6) have been proven in heat-treated samples of potassium geopolymers [52]. Crystalline phases might act as fillers to reinforce the geopolymer matrix. The presence of the crystalline phases that remained stable at high temperatures is important for the thermal stability of geopolymer. The XRD spectra of OPC paste before and after heating at 1000°C is given in figure 10 b. The XRD pics at 18° and 34° which indicated the presence of portlandite $\text{Ca}(\text{OH})_2$ disappear at 1000°C in accordance with DSC analysis. The pics of calcite (CaO) were also found in the XRD pattern of cement at 1000°C . The broad band between 32° and 33° is attributed to the C-S-H gel, the main binding product in the hydrated cement paste. This band disappears at 1000°C and the pics of allite (C3S) and belite ($\beta\text{-C}_2\text{S}$) are present in XRD spectra of heated cement paste at 1000°C . The XRD diagrams at 1000°C reveal that the main products of the C-S-H decomposition were C3S and $\beta\text{-C}_2\text{S}$, being consistent with previous reports [53–55]. Indeed, the amorphous CSH gel starts to recrystallize into $\beta\text{-C}_2\text{S}$ or C3S when the temperature exceeds 700°C [56]. The dehydration and recrystallization of CSH and CH cause their shrinkage [54]. Meanwhile, the unhydrated clinker particles, which are surrounded by CSH and CH, expand due to thermal dilation. This strain mismatch between shrinking hydration products and expanding clinker leads to micro-cracking and microstructural changes, leading to desintegration of portland cement specimen [54]. The XRD analysis of Fly ash geopolymer and portland cement pastes confirm also the stability of fly ash based geopolymer comparatively to OPC cement paste.

3.3.6 Microstructural change by SEM analysis

Microstructural images of fly ash geopolymers before and after heat exposure to 1000°C were obtained using scanning electron microscopy (SEM). Figure 11 illustrates the SEM-determined microstructure characteristics of the raw fly ash and the prepared fly ash-based geopolymers before and after heat treatment at 1000°C .

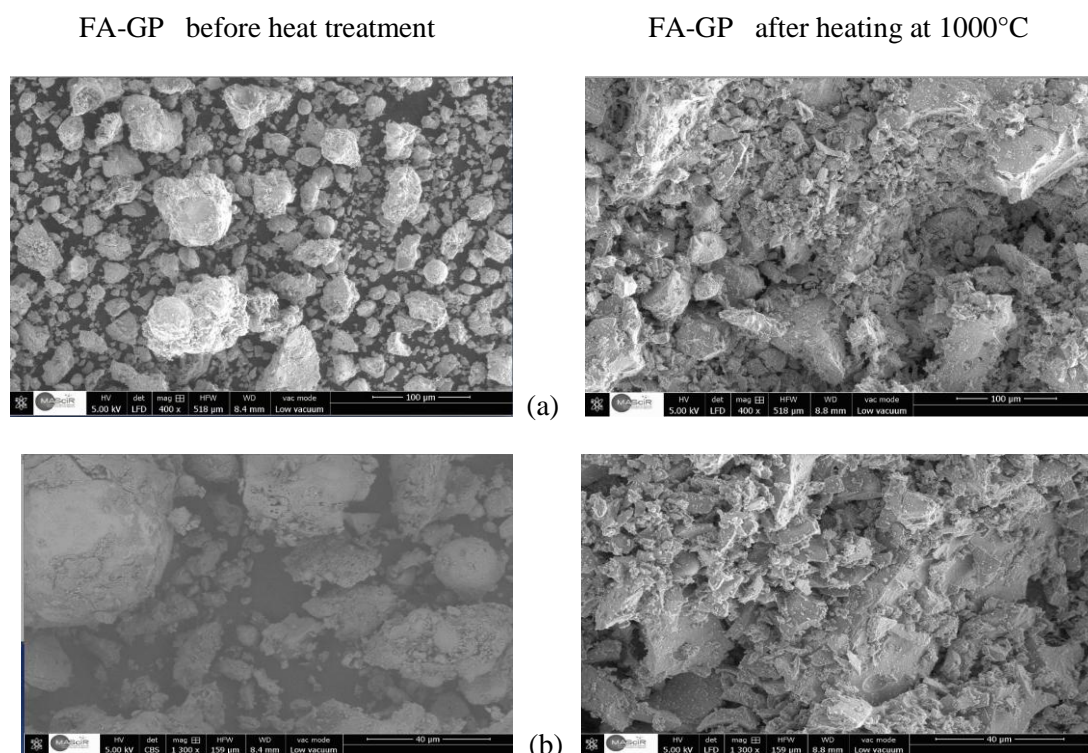


Figure 11: SEM micrographs of fly ash geopolymer before and after heat treatment at different magnification ((a) 400 magnification ; (b) 1300 magnification)

The microstructure of FA-GP before heat exposure is a porous, heterogeneous mixture of non- or partly-reacted fly ash grains, residual alkaline precipitates, pores and geopolymer gel. The geopolymer matrix seems denser after heat treatment and shows the absence of micro crack on the surface and unreacted fly ash particles. Therefore, the surface seems more homogeneous with less porosity. At elevated temperature, the rate of dissolution of the fly ash particle is enhanced and the condensation of aluminosilicate gel are obvious from the micrograph. The geopolymer matrix intervened with each other forming continuous matrix at large magnification. This suggested that there is sintering effect and partial melting due to elevated temperature. The partial melting which allowed the viscous flow to fill pores or voids present in the structure [57]. With increasing temperature exposure, the amount of residual fly ash particles became lesser and disappeared in samples heated at 1000 °C. From the SEM images, un-reacted fly ash particles shaped like hollow spheres were observable. When these shells are partially dissolved in geopolymer matrix, they appear to create a matrix with a large number of small highly dispersed pores. At elevated temperatures, these pore spaces provide escape routes for moisture in the matrix thereby decreasing the likelihood of the damage to the matrix. Some degree of sintering appears to occur at elevated temperatures, thus increasing the strength. The matrix was seemingly dense with crystalline phases, which is estimated to improve the strength of geopolymer at elevated temperature [58]. The presence of crystalline phases was confirmed by the XRD diffractogram in the section above.

Conclusion

According to the compositional and microstructural analyses, the geopolymer products derived from fly ash consist of many features: voids, pores, micro cracks, fly ash balls, dense and bulky geopolymer binders. It is considered as a hybrid mix but rather pure geopolymers. The porous microstructure proves that it is with a good fire resistant performance. The Si RMN analysis revealed that the Q4 (2Al) and Q4(3Al) units prevailed in the polysialate framework of FA-GP. The textural properties studies the FA-GP matrix is a predominantly a microporous material while the portland cement paste is predominantly a mesoporous material. This study has investigated the effect of elevated temperatures on the properties of FA-GP and OPC pastes. Geopolymer binders are well conserved after high temperature heating, it shows no cracks on the surface after high temperature exposure. The OPC samples were completely destroyed after heating at 1000°C. All geopolymers exposed to heating retained their shape up to 1000 °C without showing any destruction or dimensional change. The DSC, FT-IR and XRD analysis confirm the thermal stability of flyash based Geopolymer. The study results indicated good fire resistance of geopolymer derived from Moroccan fly ash. Further research is needed to confirm these high thermal properties. Thus, the FA-GP materials can be used as ecologically friendly fire proof building materials, sound and heat insulators.

Reference

1. Davidovits J., *World Resource Review*. 6 (2) (1994) 263.
2. Duxon P., Fernandez-Jimenez A., Provis J.L., Lukey G.C., Palomo A., Van Deventer J.S.J., *J. Mater. Sci.* 42 (2007) 2917.
3. Duxon P., Provis J.L., Lukey G.C., Van Deventer J.S.J., *Cem. Concr. Res.* 37 (2007) 1590.
4. Van Deventer J.S.J., Provis J.L., Duxon P., *Miner. Eng.* 29 (2012) 89.
5. Bakharev T., *Cem. Concr. Res.* 35 (2005) 1233.
6. Zhang J.Z., Provis J.L., Feng D., Van Deventer J.S.J., *Hazard. Mater.* 157 (2008) 587.
7. Cheng T.W., Chiu J.P., *Miner. Eng.* 16 (2003) 205.
8. Bakharev T., *Cem. Concr. Res.* 35 (2005) 658.
9. Davidovits J., *Journal of Thermal Analysis*. 37(1991)1633.
10. Davidovits J. *GEOPOLYMER Chemistry and Applications*, 4th Edition, Institut Géopolymère, (2015).
11. Xie Z., Xi Z. *Cem. Concr. Res.* 31(2001) 1245.
12. Palomo A., Grutzeck M.W., Blanco M.T., *Cem. Concr. Res.* 29 (1999) 1323.
13. Zosin A., Priimak T., Avsargov Kh., *Atomic Energy*. 85 (1) (1998) 510.
14. Davidovits J., Orlinski J. eds., *Proceedings of Geopolymer '88*, European Conference on Soft Mineralurgy, Université de Technologie, Compiègne, France, (1988).
15. Davidovits J. *First International Conference on Alkaline Cements and Concretes (1994b)* (pp. 131-149). Kiev, Ukraine.
16. Adamson R.W., A.P. Gast A.P. in *Physical chemistry of surfaces* Ch. 17, 6th ed., Wiley, New York, (1997).
17. Barrett E.P., Joyner J.G., Halenda, P.P. *J. Am. Chem. Soc.* 73 (1951) 373.

18. Lippmaa E., Mägi M., Samoson A., Engelhart G., Grimmer A .R., *J.Phys. Chem. Soc.* 88(1980) 4889.
19. Klinowski J., *Progress in NMR Spectroscopy*, 16 (1984) 237.
20. Palomo A., Grutzeck M., Blanco M. *Cem.Concr.Res.* 29 (1999)1323.
21. Derouane E. *J.Chem.Soc., Farad. Trans.* 170 (1974) 1402.
22. Farhana Z. F., Kamarudin H., Rahmat A., Al Bakri A.M.M., *Materials Science Forum*, 803 (2015) 166.
23. Metha P.K., Monterio P.J.M., *Concrete, Microstructure, Properties and Materials*, McGraw-Hill, London, (2006).
24. Barrett E.P., Joyner L.G., Halenda P.P., *J. Am. Chem. Soc.* 73 (1951) 373.
25. Powers T.C, Brownyard T.L. *ACI J. Proc.* 43 (1947) 845.
26. Juenger M.C.G., Jennings H.M. *Cem. Concr. Res.* 31 (2001) 883.
27. Mikhail R.S., Copeland E., Brunauer S., *Can. J. Chem.* 42 (1964) 426.
28. Zhang B. *Cem. Concr. Res.* 28(5) (1998) 699.
29. Asthana R., Kumar A., Dahotre N. *Materials Processing and- Manufacturing Science*, First Edition. United Kingdom: Butterworth- Heinemann. 656 p,(2006).
30. Cheng T.W., Chiu J.P. *Minerals Engineering*.16 (3) (2003) 205.
31. Alarcon-Ruiz L., Platret G., Massieu E., Ehrlacher A. *CemConcr Res.* 35(3) (2005) 609.
32. Khoury G.A., Majorana C .E., Pesavento F., Schrefler B.A. *Mag Concr Res.*54 (2)(20002) 77.
33. Skvara F., Sulc R., Tisler Z., SkricikP., Smilauer V., Zlamalov C.Z., *Ceram. Silik.* 58 (3) (2014)188.
34. Zhang H. Y., Kodur V., Qi S. L., Cao L., Wu B., *Constr. Build. Mater.* 55 (2014) 38.
35. Luna-Galiano Y., Cornejo A., Leiva C., Vilches L. F. , Fernandez-Pereira C., *Mater. Construcc.* 65(319) (2015).
36. Duan P., Yan C., Zhou W., Luo W., *Thermal. Arab. J. Sci. Eng.* 40(8) (2015) 2261.
37. Abdelalim A. M. K., Abdelaziz G. E., El-Mohr M. A. K. , Salama G.A., *Eng. Res. J.* 122(2009) 63.
38. Zhang Z., Provis J. L., Reid A., Wang H., *Constr. Build. Mater.* 56 (2014) 113.
39. Abdollahnejad Z., Pacheco-Torgal F., Felix T., Tahri W., Aguiar J. B., *Constr. Build. Mater.* 80 (2015) 18.
40. Andini S., Cioffi R., Colangelo F., Grieco T., Montag- naro F., Sanotor L., *Waste Manage.* 28 (2008) 416.
41. Mužek M. N., Zelić J., Jozić D., *Chem. Biochem. Eng. Q.* 26 (2012) 89-95.
42. Boke N., Birch G. D., Nyale S. M., Petrik L. F., *Constr. Build. Mater.* 75 (2015) 189.
43. Oudadess H., Derrien A. C., Lefloch M. J., *Therm. Anal. Calorim.* 82(2005) 323.
44. Li X., Ma X., Zhang S. , Zheng E., *Materials.* 6 (4)(2013)1485.
45. Barbosa V. F. F., MacKenzie K. J. D., Thaumaturgo C. *Int. j. inorg. chem.*2 (4) (2000) 309.
46. Alonso S., Palomo A. *CemConcr Res.* 31(1) (2001b) 25-30.
47. Granizo M. L., Alonso S., Blanco-Varela M. T., Palomo A., *J. Am. Ceram. Soc.* 85 (2002) 225-231.
48. Rovnaník P., Safrankova K. *Materials* .9 (2016) 535.
49. Choi Y.C., Kim J.H., Choi S., *Asian J. Chem.* 26 (17) (2014) 5517.
50. Li X., Ma X., Zhang S., Zheng E., *Materials.* (6) (4)(2013) 1485.
51. Barbosa, V. F. F., MacKenzie, K. J. D., Thaumaturgo C., *Inter J Inorg Mater.* 2(4)(2000) 309.
52. Barbosa V.F.F., Mac Kenzie K.J.D. *Mater. Lett.* 57(2003) 1477.
53. Taylor HFW. *Cement chemistry*. New York, USA: Academic Press, 1990.
54. Piasta J, Sawics Z, Rudzinski L., *Mater Struct* .17 (1984) 291.
55. Neville AM. *Properties of concrete*. Harlow, England: Longman Group Limited; 1995.
56. Macclune WF (1980) *Mineral powder diffraction file*. JCPDS, Swarthmore
57. Rahier H., Wastials J. Biesemans M., Willem R., Van Assche G., Van Mele B., *J. Mater. Sci.* 42 (2007) 9282.
58. He P., Jia D., Wang S. J., *Eur. Ceram. Soc.* 33 (2013) 689.

(2017) ; <http://www.jmaterenvirosci.com>